Lesion Localization in Paediatric Epilepsy Using Patch-Based Convolutional Neural Network

Azad Aminpour[1], Mehran Ebrahimi[1(✉)], and Elysa Widjaja[2]

[1] Ontario Tech University, Oshawa, ON L1G 0C5, Canada
{azad.aminpour,mehran.ebrahimi}@ontariotechu.net
[2] The Hospital for Sick Children (SickKids), Toronto, ON M5G 1X8, Canada
elysa.widjaja@sickkids.ca

Abstract. Focal Cortical Dysplasia (FCD) is one of the most common causes of paediatric medically intractable focal epilepsy. In cases of medically resistant epilepsy, surgery is the best option to achieve a seizure-free condition. Pre-surgery lesion localization affects the surgery outcome. Lesion localization is done through examining the MRI for FCD features, but the MRI features of FCD can be subtle and may not be detected by visual inspection. Patients with epilepsy who have normal MRI are considered to have MRI-negative epilepsy. Recent advances in machine learning and deep learning hold the potential to improve the detection and localization of FCD without the need to conduct extensive pre-processing and FCD feature extraction. In this research, we apply Convolutional Neural Networks (CNNs) to classify FCD in children with focal epilepsy and localize the lesion. Two networks are presented here, the first network is applied on the whole-slice of the MR images, and the second network is taking smaller patches extracted from the slices of each MRI as input. The patch-wise model successfully classifies all healthy patients (13 out of 13), while 12 out of 13 cases are correctly identified by the whole-slice model. Using the patch-wise model, we identified the lesion in 17 out of 17 MR-positive subjects with coverage of 85% and for MR-negative subjects, we identify 11 out of 13 FCD subjects with lesion coverage of 66%. The findings indicate that convolutional neural network is a promising tool to objectively identify subtle lesions such as FCD in children with focal epilepsy.

Keywords: Focal Cortical Dysplasia · Convolutional Neural Network · Deep learning · Patch-based

1 Introduction

Epilepsy is a common neuroulogical disorder which has devastating consequences on children's quality of life. It has an incidence rate of 4 to 9 in 1000 per year in paediatric patients [8,9]. Despite advances in the treatment of epilepsy, approximately 30% of patients with epilepsy continue to have seizures refractory to

A. Campilho et al. (Eds.): ICIAR 2020, LNCS 12132, pp. 216–227, 2020.
https://doi.org/10.1007/978-3-030-50516-5_19

medications [17,21,23]. Prolonged uncontrolled epilepsy has detrimental effects on the neurodevelopment of a child due to brain injury [20].

For patients with medically intractable epilepsy surgery may be the best option to achieve seizure freedom [6,24,26]. In this case, a comprehensive pre-surgical evaluation to detect the lesion responsible for epilepsy is necessary. Magnetic Resonance Imaging (MRI) plays an essential role in the pre-surgical workup of children with epilepsy in order to identify an underlying lesion responsible for the epilepsy [7,21]. The detection of a lesion on MRI varies in the literature and ranges from 30% to 85% of patients with refractory focal epilepsy [10]. Failure to identify a lesion on MRI will result in a lower likelihood of epilepsy surgery, increased use of invasive electroencephalography monitoring for surgical planning, and lower odds of seizure-free surgery outcome. For instance, the surgical outcome is considerably better in patients with an identifiable lesion than patients in whom the lesion cannot be identified.

Focal cortical dysplasia (FCD) is a brain malformation and one of the most common lesions responsible for medically intractable focal epilepsy in children. The incidence of FCD in those with intractable partial epilepsy ranges from 10% to 12% in combined paediatric and adult series, and up to 26% in paediatric patients alone [13]. The MRI features of FCD are frequently subtle, and may not be detected by visual assessment in up to 50% to 80% of patients with medically intractable epilepsy. The MRI features of FCD include cortical thickening, abnormal signal in the white and/or gray matter, blurring of the gray-white matter junction, and abnormal sulcal pattern [2,16]. Patients with MRI-visible FCD are considered to have MR-positive FCD. These patients may have one or more of these FCD features identifiable on the MRI, while others may demonstrate more. In some patients FCD may not be detected on MRI; these patients are considered to have MR-negative epilepsy [2,16].

A neuroradiologist performs most pre-surgery lesion localization through examining the patient's MRI scan. However, visual assessment of MRI is subjective and highly dependent on the expertise of the observer. Therefore, there is a need for a more advanced and objective tool for analyzing the MRI data. Image processing algorithms offer the potential to detect subtle structural changes, which may not be identifiable on visual inspection of MRI. Existing image processing methods to identify FCD based on the MRI features are limited in their ability as they are mostly based on extracting and detecting specific features of FCD. Recently, artificial intelligence (AI) techniques based on deep neural networks have emerged and been applied to many fields, including various areas of medicine. Deep learning methods' success motivates us to apply deep learning-based techniques to provide the neuroradiologists with means for lesion localization.

2 Literature Review

Due to the importance of FCD detection for pre-surgery evaluation, numerous works [1–5,11,12,14–16,18] have been proposed to help neuroradiologists better

detect and localize FCD. The published works are mostly considering adult cases while a few studies [1,16] have concentrated on identifying FCD in children with focal epilepsy.

Most of the methods mentioned above are based on extracting MRI features which are fed into a classifier. Morphometry features are among the most common features that have been used, for example, Martin et al. in 2015 [18] utilized voxel-based morphometry (VBM) along with surface-based morphometry (SBM) for better identification of FCD. Other works considered morphometric features and textural features together [4,5]. Besson et al. performed an automatic detection by utilizing a two-step classification, a neural network trained on manual labels followed by a fuzzy k-Nearest Neighbor classifier (fkNN) to remove false positive clusters [5]. In another research, textural and structural features were used to develop a two-stage Bayesian classifier [2]. Most studies utilizing computer aided tools to identify a lesion in patients with medically intractable epilepsy have been conducted in adults with fully developed brain. The immature brain in children may present additional challenges for detecting FCD on images.

There is limited research evaluating paediatric FCD, [1,16] are two of the most recent ones. Adler et al. utilized morphometric and structural features for training a neural network. Post-processing methods such as the "doughnut" method - which quantifies local variability in cortical morphometry/MRI signal intensity, and per-vertex interhemispheric asymmetry has also been developed in [1]. Kulaseharan et al. in 2019 [16] combined morphometric features and textural analysis using Gray-Level Co-occurrence Matrices (GLCM) on MRI sequences, to detect FCD in paediatric cases. A modified version of the 2-Step Bayesian classifier method proposed by Antel et al. [2] is applied and trained on textural features derived from T1-weighted (T1-w), T2-weighted (T2-w), and FLAIR (Fluid Attenuated Inversion Recovery) sequences. The authors correctly identified 13 out of 13 of healthy subjects and localized lesions in 29 out of 31 of the MR-positive FCD cases with 63% coverage of the complete extent of the lesion. The method also co-localized lesions in 11 out of 23 of the MR-negative FCD cases with coverage of 31%.

A common feature of all these studies for FCD detection is that they are based on extracted MRI features where, through analysis software and image processing techniques, a feature vector is constructed for a patch or a voxel in the MR sequence. Later each feature vector is classified using a classifier. In this research, we propose to implement a CNN, which is applied directly on the MR sequences. More recently, two studies have utilized a deep learning approach to detect FCD [3,12].

Gill et al. in 2018 [12] trained two networks on patches extracted from patients' MR sequences with histologically-validated FCD. The algorithm was trained on multimodal MRI data from a single site and evaluated on independent data from seven sites (including the first site) worldwide for a total of 107 subjects. Both networks had a similar structure where they included three stacks of convolution and max-pooling layers with 48, 96 and 2 feature channels and

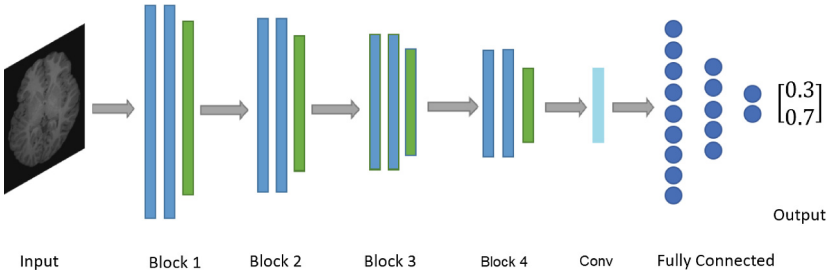

Fig. 1. Whole-slice network architecture, blue rectangles are convolutional layers, and green ones are pooling layers, columns of circles are representing fully connected layers. The light blue rectangle is a 1×1 convolutional layer while the other convolutional layers are 3×3. (Color figure online)

$3 \times 3 \times 3$ kernels. The first network is trained to maximize recognized lesional voxels, while the second network is trained to reduce the number of misclassified voxels (i.e., removing false positives while maintaining optimal sensitivity) [12]. Later in 2019, David et al. [3] developed a CNN for FCD detection. The proposed network is trained on T1 weighted and FLAIR. In this work to overcome the limited number of training data, authors utilized a conditional Generative Adversarial Network (cGAN) to compose synthetic data where it is used in training the CNN along with the real data [3]. They trained and evaluated their model on 42 cases with FCD and 56 healthy controls. The method classified 54 out of 56 healthy control cases as normal and detected 39 out of 42 FCD cases as FCD.

In this study, our aim was to develop a model where it takes an MRI and decides whether it has FCD or not, and in the case of FCD, it will localize the region of abnormal tissue. Our work is different from previous studies with deep learning on two main parts. First, we are only considering paediatric FCD which means we train and evaluate our model only on paediatric patients. Gill et al. [12] are considering both adult and paediatric data and David et al. [3] are focusing on adult cases. Second, both works have considered subject classification where they report if an input case has FCD or not. In this work, in addition to subject-wise classification, we localize the lesion in the FCD subjects.

3 Method

We apply a specific type of deep learning networks known as Convolutional Neural Networks (CNN) to classify MRI of FCD patients and localize the responsible lesion in the image. As processing the two-dimensional data will be faster than the three-dimensional ones, we will consider presenting slices of the 3D MR data as 2D inputs to our network. To this end, we choose 2D slices extracted from the MRI volume as the first set of inputs and later, each slice was partitioned into smaller patches that was used as the second set of inputs. At the end, each

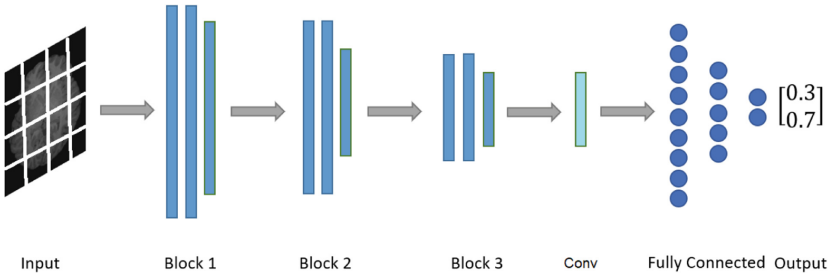

Fig. 2. Patch-wise Network Architecture, blue rectangles are convolutional layers, and columns of circles are representing fully connected layers. The light blue rectangle is a 1×1 convolutional layer while the other convolutional layers are 3×3. (Color figure online)

volume was given to a neuroradiologist in order to detect and segment the lesion. We proposed two networks based on the two sets of inputs.

The first proposed model is a two-class classifier that takes two-dimensional slices out of 3D MR data and classifies the slice as FCD or healthy. We trained the network on our data where a slice is labelled as FCD if at least one pixel is lesional; otherwise, it is considered to be healthy. The proposed whole-slice CNN has two parts, a feature extraction part and a classification part.

The feature extraction part of the network consists of four blocks of two convolution layers, followed by a Max-Pooling layer. The blocks are followed by one convolutional layer at the end. The classification part consists of three fully connected layers which produces a vector with two elements representing the probability of each class. Therefore in total, there are nine Convolutional layers, four Max-Pooling layers and three Fully connected layers. The architecture is illustrated in Fig. 1. We implemented the Relu activation function after each layer except for the last fully connected layer, where we used Softmax instead. Also, the output of each layer was normalized using batch normalizer and to prevent overfitting, the dropout technique was applied.

In our early experiments, we realized that our model tends to over-fit toward the healthy slices. This was the result of the higher number of healthy slices compared to lesional slices. The unbalanced data distribution is a common problem in FCD detection and segmentation [12]. To overcome this problem, we reduced the number of healthy slices as we were not able to generate more lesional slices. First, we considered slices that contain more than 10% foreground pixels. In other words, we discarded the first few and several end slices containing mostly background/air. Then, we sampled the same number of healthy slices as lesional slices from all healthy slices and performed the training. The sampling process is random; however, it is weighted toward slices, which contain more brain tissue pixels.

One of the problems in the slice level classifier is that the lesion segment is smaller compared to healthy brain tissue. In the process of generating ground

truth labels for the training slices, we labelled a slice as lesional if it included at least one lesional pixel. Such labelling process may cause an error in the framework as the network can treat a slice where a large portion of it is healthy as lesional. To overcome this problem, we partitioned each slice into smaller patches and trained the network on the new training set.

The patch-wise network architecture as shown in Fig. 2 is similar to the whole-slice network. We have three blocks of convolutional layers followed by three fully connected layers. In the patch-wise network, we are using convolution layers instead of Max-pooling layers at the end of each block. These layers are equipped with a filter of size 2×2 that slides by a stride of size two, which produces an output half the size of the input. The advantage of the convolution layer over the Max-pooling layer is that the network is able to learn filters' weights for "better" downsampling [19,25]. Overall, the network has ten convolution layers and three fully connected layers. We utilized ReLu activation on all layers except the last layer, which is using Softmax. Furthermore, we normalized the output of each layer using batch normalizer and to prevent over-fitting, we applied dropout on fully connected layers.

In the patch-wise network, we label each patch with two labels, FCD or healthy. Again, we labelled a patch as FCD if at least one pixel is lesional. As we partitioned each slice into smaller patches, we ended up with patches only containing background/air or a small portion of healthy tissue, which we omitted from our training. We controlled the healthy patch selection with one parameter, percent of valued pixels relative to air/background. Here we selected patches with more than 20% valued pixels.

In our evaluation, we faced a similar challenge as the whole-slice classifier where our model was predicting every patch as healthy. Therefore, we tune the healthy patch selection parameter and change it to 50% (patches with more than 50% valued pixels). Also, we performed sampling when selecting the healthy patches for training. The sampling is random but with higher probability of patches with greater number of valued pixels. The next parameter to tune is the patch size which we explored 100×100, 50×50, and 25×25. We picked 50×50 patch sizes as it outperformed others in our preliminary experiments. Patch size was selected independent of the lesion size as the lesion segment has various sizes across all subjects. In the partitioning step, we examine both stride and non-stride version of the patch extraction. The non-stride partitioning simply means to partition the slice into patches of the same size where they don't overlap. For the case of stride, we also consider an overlap between patches to take into account every possible local information in the slice. We applied stride of 25 on the 50×50 patch selection and trained both networks on their corresponding dataset. The stride of 25 ensures that we have covered every point twice without increasing redundant training data. Larger strides will result in missing portions of the image and smaller strides will generate a lot of patches covering the same area which makes the training time longer.

4 Result

Our dataset contains T1 MRI volumes of paediatric subjects. It includes 30 FCD diagnosed subjects (17 MR-positive and 13 MR-Negative) and 13 healthy controls. The data is in the form of DICOM images and required several preprocessing steps including brain extraction, re-orientation, and resizing to a standard size. The brain extraction part is done utilizing the BET (Brain Extraction Tool) algorithm proposed by Smith et al. in 2002 [22]. Since CNN is taking images of the same size, every slice in our data needed to be resized to a standard size. We zero-padded the smaller slices while cutting background/air part of the larger slices to a size of 400×300. Due to the sensitive nature of our data, we avoided shrinking or stretching the data to resize them. At the end, 'clean' data was presented to a neuroradiologist to segment the lesion in FCD subjects, which is used as ground truth in our training and evaluation.

In both whole-slice and patch-wise models, each network was trained and evaluated using the leave-one-out technique. This means the network was trained on all of the available data except for the one used for evaluation. We repeated the experiment 30 times, which is the same as the number of FCD subjects. The output of each network is a label that identifies if the input slice or patch is lesional or healthy. Then based on the ratio of predicted lesional patches (or slices) over the number of predicted healthy patches (or slices), we will decide if the subject is lesional or healthy. We have quantified our results using lesional sensitivity, which is the true positive (TP) rate and lesional specificity, which is the true negative (TN) rate. Here true positive means number of healthy patches (or slices) classified as healthy, and true negative refers to the number of lesional patches (or slices) classified as lesional. We also reported subject-wise sensitivity and specificity which indicates the number of healthy or FCD subjects classified as healthy or FCD respectively.

The result of the whole-slice network is presented in Table 1. The model identified 12 out of 13 healthy control subjects. In the case of FCD subjects, the whole slice network failed to classify one of the MR-Positive cases while localized the lesion in the other 16 subjects with an average coverage of 54%. For MR-Negative cases, 11 out of 13 subjects were detected with an average coverage of 56%. The result for the patch-wise network is presented in Tables 2 and 3. Each row represents one experiment where we train the network using patches extracted from slices within all subjects except for the subject relating to its row.

Table 1. Whole-slice two class classifier results

	MR-positive	MR-negative
Subject-wise sensitivity	0.92	0.92
Subject-wise specificity	0.94	0.85
Lesional sensitivity	0.59	0.72
Lesional specificity	0.54	0.56

Table 2. 2D patch-wise two class classifier results for lesional subjects

Test sample	Train accuracy	Test accuracy	Sensitivity	Specificity	Subject label
MR-positive subjects					
4	99%	99%	1.00	0.87	1
5	99%	99%	1.00	0.70	1
8	99%	99%	1.00	0.81	1
10	99%	99%	1.00	0.89	1
13	99%	99%	1.00	0.85	1
18	99%	99%	1.00	0.86	1
20	99%	99%	1.00	0.92	1
21	99%	99%	1.00	0.85	1
22	99%	99%	1.00	0.87	1
23	99%	99%	1.00	0.86	1
24	99%	99%	1.00	0.84	1
26	99%	99%	1.00	0.88	1
27	99%	99%	1.00	0.78	1
29	99%	99%	1.00	0.89	1
35	99%	99%	1.00	0.86	1
36	99%	99%	1.00	0.86	1
39	99%	99%	1.00	0.86	1
Average	99%	99%	1.00	0.85	
MR-negative subjects					
1	99%	99%	1.00	0.78	1
2	99%	99%	1.00	0.67	1
3	99%	97%	1.00	0.55	0
7	99%	98%	1.00	0.47	0
9	99%	95%	1.00	0.66	1
11	99%	99%	1.00	0.75	1
12	99%	99%	1.00	0.74	1
16	99%	99%	1.00	0.69	1
17	99%	94%	1.00	0.63	1
19	99%	95%	1.00	0.64	1
31	99%	94%	1.00	0.54	1
32	99%	95%	1.00	0.64	1
38	99%	99%	1.00	0.83	1
Average	99%	97%	1.00	0.66	

The first column is the test subject, the second and third columns are training and test accuracy, which are the percentage of correctly predicted patches in training and evaluation set. We cannot solely rely on training/test accuracy as

Table 3. 2D patch-wise two class classifier results for healthy controls. We cannot report the lesional specificity as we do not have any lesional patches in our data. Zeros in the last column mean that the test subject is being classified as healthy.

Test sample	Train accuracy	Test accuracy	Sensitivity	Specificity	Subject label
30	99%	99%	1.00	N/A	0
51	99%	99%	0.99	N/A	0
52	99%	99%	1.00	N/A	0
53	99%	99%	1.00	N/A	0
54	99%	99%	1.00	N/A	0
55	99%	99%	1.00	N/A	0
56	99%	99%	1.00	N/A	0
57	99%	99%	1.00	N/A	0
58	99%	99%	1.00	N/A	0
60	99%	99%	1.00	N/A	0
61	99%	99%	1.00	N/A	0
62	99%	99%	1.00	N/A	0
63	99%	99%	1.00	N/A	0
Average	99%	99%	1.00		

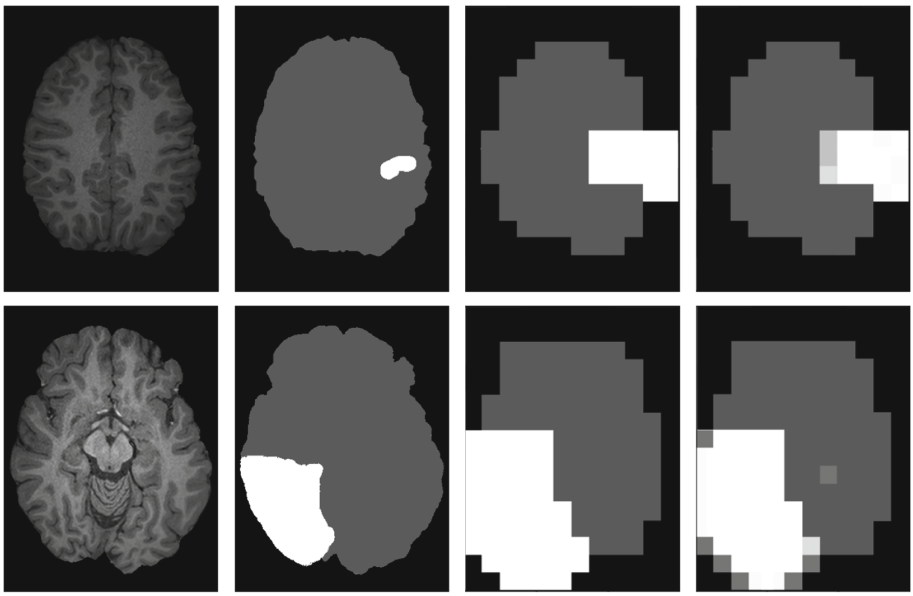

Fig. 3. Patch-wise model output; from left to right, columns represent the original slice, pixel-wise ground-truth, patch-wise ground-truth, patch-wise network prediction.

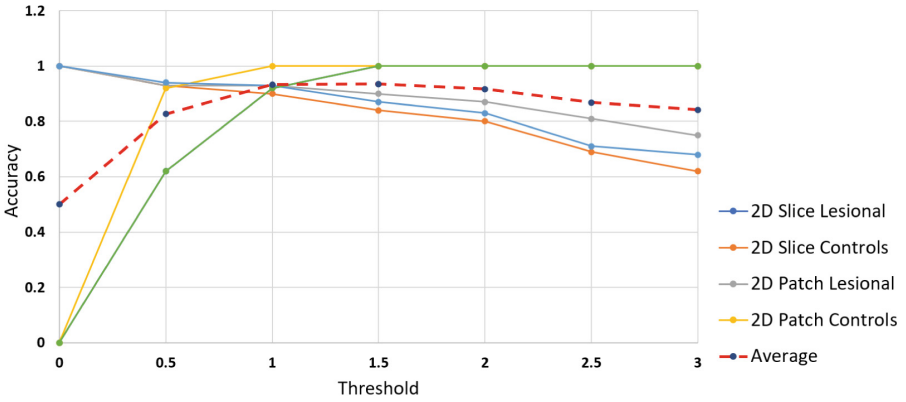

Fig. 4. Subject class label threshold, horizontal axis shows the threshold and the vertical axis indicates the accuracy for lesional and control subjects.

a measure of how well the network is performing since high numbers may be a result of high number of correctly classified healthy patches. Two complete the table, lesional sensitivity and specificity are reported in the next two columns.

The results for FCD approved patients are presented in Table 2. The first block is the MR-positive subjects, where we can see the network detected all 17 out of 17 cases with 85% coverage. The second portion is the MR-negative subjects' results. The model detected 11 out of 13 cases with a coverage of 66%. The large variation of the specificity (47%–83%) in Table 2 for MR-negative subjects can be attributed to lack of visual features which makes the training and evaluation for MR-Negative subjects more difficult. In Table 3, the results for 13 healthy control cases are reported where we successfully classified all 13 as healthy. The patch-wise network output along with the pixel-level and patch-level ground truth is illustrated in Fig. 3. Each row represents a patient, the top row is a patient with MR-positive FCD and the bottom is an MR-negative FCD approved subject. First image in each row is the actual slice, next one is the pixel-wise ground truth provided by a neuroradiologist, followed by the patch ground truth extracted from the pixel-wise ground truth, and the network prediction. As it is obvious the network's output localized the lesion in both subjects with acceptable accuracy.

In both models, we consider a subject prediction class as healthy or lesional by finding the number of predicted lesional patches (or slices) over the number of predicted healthy patches (or slices). If this ratio is larger than one percent, we consider the subject as lesional, otherwise it is considered as healthy. Selecting the right threshold is important as it decides whether a patient has FCD or not. We examined several options for each network and, to stay consistent in all experiments we plotted the results in Fig. 4. Lesional accuracy here is the average of MR-positive and MR-negative accuracy. The red curve in the graph is the average for all accuracies given the specific threshold. The curve is maximum at one. Hence, we chose one as a universal threshold for all of our experiments.

5 Conclusion and Future Work

We explored the problem of FCD lesion detection and localization in paediatric patients, a challenging lesion localization task that is typically performed by visual assessment of the patients' MRI. We applied two CNNs which were trained and evaluated on paediatric subjects' data. Our patch-wise model successfully classified all healthy patients (13 out of 13). We identified the lesion in 17 out of 17 MR-positive subjects with a lesion coverage of 85% and for the MR-negative subjects, we correctly identified 11 out of 13 subjects with lesion coverage of 66% using the patch-wise network. These findings indicate that CNN is a promising tool to identify subtle FCD lesions in children with focal epilepsy. Future work will include using three-dimensional patches in the model and integrating additional imaging modalities to improve lesion localization.

Acknowledgments. This research was conducted with the support of EpLink – The Epilepsy Research Program of the Ontario Brain Institute (OBI). The opinions, results and conclusions are those of the authors and no endorsement by the OBI is intended or should be inferred. This research was also supported in part by an NSERC Discovery Grant for M.E. AA would like to acknowledge Ontario Tech university for a doctoral graduate international tuition scholarship (GITS). The authors gratefully acknowledge the support of NVIDIA Corporation for the donation of GPUs used in this research through its Academic Grant Program.

References

1. Adler, S., et al.: Novel surface features for automated detection of focal cortical dysplasias in paediatric epilepsy. NeuroImage: Clin. **14**, 18–27 (2017)
2. Antel, S.B., et al.: Automated detection of focal cortical dysplasia lesions using computational models of their MRI characteristics and texture analysis. Neuroimage **19**(4), 1748–1759 (2003)
3. Bastian, D., et al.: Conditional generative adversarial networks support the detection of focal cortical dysplasia. Organization for Human Brain Mapping (2019, Abstract Submission)
4. Bernasconi, A., et al.: Texture analysis and morphological processing of magnetic resonance imaging assist detection of focal cortical dysplasia in extra-temporal partial epilepsy. Ann. Neurol.: Off. J. Am. Neurol. Assoc. Child Neurol. Soc. **49**(6), 770–775 (2001)
5. Besson, P., Bernasconi, N., Colliot, O., Evans, A., Bernasconi, A.: Surface-based texture and morphological analysis detects subtle cortical dysplasia. In: Metaxas, D., Axel, L., Fichtinger, G., Székely, G. (eds.) MICCAI 2008. LNCS, vol. 5241, pp. 645–652. Springer, Heidelberg (2008). https://doi.org/10.1007/978-3-540-85988-8_77
6. Bourgeois, M., Di Rocco, F., Sainte-Rose, C.: Lesionectomy in the pediatric age. Child's Nerv. Syst. **22**(8), 931–935 (2006)
7. Centeno, R.S., Yacubian, E.M., Sakamoto, A.C., Ferraz, A.F.P., Junior, H.C., Cavalheiro, S.: Pre-surgical evaluation and surgical treatment in children with extratemporal epilepsy. Child's Nerv. Syst. **22**(8), 945–959 (2006)

8. Chin, R.F., Neville, B.G., Peckham, C., Bedford, H., Wade, A., Scott, R.C., et al.: Incidence, cause, and short-term outcome of convulsive status epilepticus in childhood: prospective population-based study. Lancet **368**(9531), 222–229 (2006)
9. Coeytaux, A., Jallon, P., Galobardes, B., Morabia, A.: Incidence of status epilepticus in french-speaking switzerland (EPISTAR). Neurology **55**(5), 693–697 (2000)
10. Colombo, N., et al.: Focal cortical dysplasias: MR imaging, histopathologic, and clinical correlations in surgically treated patients with epilepsy. Am. J. Neuroradiol. **24**(4), 724–733 (2003)
11. Gill, R.S., et al.: Automated detection of epileptogenic cortical malformations using multimodal MRI. In: Cardoso, M.J., et al. (eds.) DLMIA/ML-CDS -2017. LNCS, vol. 10553, pp. 349–356. Springer, Cham (2017). https://doi.org/10.1007/978-3-319-67558-9_40
12. Gill, R.S., et al.: Deep convolutional networks for automated detection of epileptogenic brain malformations. In: Frangi, A.F., Schnabel, J.A., Davatzikos, C., Alberola-López, C., Fichtinger, G. (eds.) MICCAI 2018. LNCS, vol. 11072, pp. 490–497. Springer, Cham (2018). https://doi.org/10.1007/978-3-030-00931-1_56
13. Hader, W.J., et al.: Cortical dysplastic lesions in children with intractable epilepsy: role of complete resection. J. Neurosurg.: Pediatrics **100**(2), 110–117 (2004)
14. Huppertz, H.J., et al.: Enhanced visualization of blurred gray-white matter junctions in focal cortical dysplasia by voxel-based 3D MRI analysis. Epilepsy Res. **67**(1–2), 35–50 (2005)
15. Hutton, C., De Vita, E., Ashburner, J., Deichmann, R., Turner, R.: Voxel-based cortical thickness measurements in MRI. Neuroimage **40**(4), 1701–1710 (2008)
16. Kulaseharan, S., Aminpour, A., Ebrahimi, M., Widjaja, E.: Identifying lesions in paediatric epilepsy using morphometric and textural analysis of magnetic resonance images. NeuroImage: Clin. **21**, 101663 (2019)
17. Kwan, P., Brodie, M.J.: Early identification of refractory epilepsy. N. Engl. J. Med. **342**(5), 314–319 (2000)
18. Martin, P., Bender, B., Focke, N.K.: Post-processing of structural MRI for individualized diagnostics. Quant. Imaging Med. Surg. **5**(2), 188 (2015)
19. Nazeri, K., Aminpour, A., Ebrahimi, M.: Two-stage convolutional neural network for breast cancer histology image classification. In: Campilho, A., Karray, F., ter Haar Romeny, B. (eds.) ICIAR 2018. LNCS, vol. 10882, pp. 717–726. Springer, Cham (2018). https://doi.org/10.1007/978-3-319-93000-8_81
20. Pitkänen, A., Sutula, T.P.: Is epilepsy a progressive disorder? Prospects for new therapeutic approaches in temporal-lobe epilepsy. Lancet Neurol. **1**(3), 173–181 (2002)
21. Rastogi, S., Lee, C., Salamon, N.: Neuroimaging in pediatric epilepsy: a multimodality approach. Radiographics **28**(4), 1079–1095 (2008)
22. Smith, S.M.: Fast robust automated brain extraction. Hum. Brain Mapp. **17**(3), 143–155 (2002)
23. Snead III, O.C.: Surgical treatment of medically refractory epilepsy in childhood. Brain Dev. **23**(4), 199–207 (2001)
24. Spencer, S., Huh, L.: Outcomes of epilepsy surgery in adults and children. Lancet Neurol. **7**(6), 525–537 (2008)
25. Springenberg, J.T., Dosovitskiy, A., Brox, T., Riedmiller, M.: Striving for simplicity: the all convolutional net. arXiv preprint arXiv:1412.6806 (2014)
26. Wyllie, E.: Surgical treatment of epilepsy in children. Pediatr. Neurol. **19**(3), 179–188 (1998)